Single-active-electron approximation for describing molecules in ultrashort laser pulses and its application to molecular hydrogen

Manohar Awasthi, Yulian V. Vanne, and Alejandro Saenz
AG Moderne Optik, Institut für Physik, Humboldt-Universität zu Berlin, Hausvogteiplatz 5-7, D-10 117 Berlin, Germany

Alberto Castro
Institut für Theoretische Physik, Freie Universität Berlin, Arnimallee 14, D-14 195 Berlin, Germany

Piero Decleva
Dipartimento di Scienze Chimiche, Universitá di Trieste, Via L. Giorgieri 1, I-34127 Trieste, Italy
(Received 10 October 2007; revised manuscript received 7 March 2008; published 3 June 2008)

A numerical approach that allows for the solution of the time-dependent Schrödinger equation (TDSE) describing molecules exposed to intense short laser pulses was developed. The molecular response to the strong field is described within the single-active electron approximation (SAE). The method is applied in the fixed-nuclei approximation to molecular hydrogen with parallel orientation of the internuclear axis to the laser field. The validity of the SAE is investigated by comparing the ionization and electronic excitation yields to full two-electron solutions of the TDSE. The present results are also used to investigate the validity of approximate SAE methods like the molecular Ammosov-Delone-Krainov and the strong-field approximation.

DOI: 10.1103/PhysRevA.77.063403 PACS number(s): 33.80.Rv

I. INTRODUCTION

Molecules exposed to intense laser fields show a number of effects that are necessarily absent in atoms. This includes phenomena like, e.g., bond softening, bond hardening (also called light-induced states), enhanced ionization at some critical internuclear separation, and above-threshold dissociation (see [1] and references therein). Furthermore, the ionization behavior of molecules even in the absence of the mentioned effects can differ from the atomic one due to the multicentered, nonspherical symmetry of the molecular potential. This can lead to a pronounced dependence of the ionization process on the molecular orientation (and thus the rotational state) or to interference effects due to the electron emission from different atomic centers [2–6]. A possible dependence of the ionization rate on the nuclear geometry can on the other hand result in a dependence on the vibrational state and wave function [7–11].

While it is expected that the mentioned differences between atomic and molecular systems should show up most clearly, if differential ionization yields like energy and especially angular resolved photoelectron spectra are considered, already the total ionization yield indicates purely molecular effects. According to simple strong-field ionization models like the Ammosov-Delone-Krainov (ADK) approximation [12] the ionization rate depends mostly on the ionization potential. However, it was experimentally discovered that a large number of molecules appear to be more stable in laser fields than atoms with a comparable ionization potential [13–16]. This phenomenon was termed *suppressed ionization*.

An extension of very popular models for describing atoms in strong fields [the strong-field approximation (SFA) and the ADK model] to the molecular case using molecular orbitals (MO) leads to the so called MO-SFA [2] and MO-ADK [17] models that both are capable of correctly predicting the occurrence or absence of suppressed ionization for a number of molecular systems. There are, however, evident differences in the quantitative description of the predicted suppression ratios as well as their dependence on laser-pulse parameters [18]. Furthermore, the MO-SFA results are rather strongly gauge dependent, i.e., the predictions obtained in length (LG) or velocity gauge (VG) differ substantially. This includes not only a quantitative deviation (easily by two or three orders of magnitude due to the problem of correctly incorporating the Coulomb correction), but in some cases also qualitative ones. One possible example is the ionization rate for parallel or perpendicular orientation of a nitrogen molecule with respect to laser polarization. In [19,20] it was found that velocity and length gauge predict the perpendicular or parallel orientation, respectively, to possess higher ionization rates. Note, however, that a different result is found for MO-SFA-VG in [21,22]. In many other cases the existing experimental data are not sufficient to allow for a clear answer which of the proposed models (MO-ADK, MO-SFA-LG, or MO-SFA-VG) is most appropriate. Very recently, it was even argued that for molecules SFA-LG should be formulated in a different way than was previously done in deriving the MO-SFA-LG [23].

A common feature of the molecular strong-field ionization models mentioned so far is that they all rely on the single-active-electron approximation (SAE). Within the SAE ionization is described as a pure one-electron process in which all remaining (nonejected) electrons act as frozen spectators. In view of the rather large and partially even qualitative differences between the predictions of the different SAE-based approximations it is evidently of great importance to develop an approach that allows one to describe molecular systems exposed to intense short laser pulses in a way that is free of the further approximations introduced, e.g., by MO-ADK or SFA. This work reports the development of such a method. The time-dependent Schrödinger equation (TDSE) describ-

ing a molecular system exposed to a laser pulse is solved within the SAE. Therefore the method is named SAE-TDSE. In contrast to SFA the present approach is gauge independent. Most importantly, the Coulomb interaction between the ejected electron and the remaining ion is automatically included in the SAE-TDSE while in the SFA it is only semiempirically (VG) or usually not at all (LG) considered.

The range of validity with respect to laser parameters is also in principle unlimited in the case of the SAE-TDSE. This is a further advantage compared to MO-SFA and especially the pure tunneling model MO-ADK. SAE-TDSE provides thus a tool for the quantitative treatment of the strong-field ionization behavior (including, e.g., high-harmonic generation) as well as for the investigation of the applicability and validity of simpler SAE-based models like MO-SFA and MO-ADK. Furthermore, SAE-TDSE delivers also information on the excitation of bound electronic states in a laser pulse. These states and their possible population are by construction completely ignored in MO-ADK and MO-SFA.

An intrinsic ambiguity of SAE is introduced by the description of the potential created by that part of the atomic or molecular system that does not respond to both the laser field and the change of the potential due to the active electron that responds to the laser field. Since electrons are indistinguishable, the need for an artificial distinction between the active electron and the inactive ones necessarily leads to formal inconsistencies as was discussed, e.g., in [24]. Besides model potentials, mean-field theories that yield orbitals allow one to implement SAE in the most straightforward way. Therefore mostly Hartree-Fock (HF) theory was used in the implementation of SAE in the context of MO-ADK or MO-SFA. Freezing all but one electron leads then to a frozen-core HF (static-exchange) description. In the present SAE-TDSE implementation a different approach was chosen by describing the inactive electrons with the aid of density-functional theory (DFT). The advantage compared to HF theory is the ability to include in an approximate way correlation in the description of the inactive electrons. The price to pay is the unknown exact functional. In this work on molecular hydrogen the results obtained for DFT and HF theory are directly compared to each other.

The applicability of the SAE in which the relaxation of the remaining electrons as well as the action of the laser field on them is completely ignored is so far unclear. The success of the SAE-TDSE applied to atoms (being pioneered in [25]) as is demonstrated, e.g., in [26–28] seems to indicate that very often intense laser fields primarily act on isolated electrons. This is further substantiated by the success of the SAE-based SFA for a large number of atoms and laser parameters reported, e.g., in [29]. Clearly, SAE fails, if doubly excited states are important. For systems with delocalized π electrons nonadiabatic multielectron behavior was discussed in [30]. The SAE has recently also been explicitly criticized. A formal criticism and suggestion for an improvement is given in [24], while it was argued that only a many-electron tunneling model can describe suppressed ionization in fullerenes in [31]. However, it was thereafter demonstrated that at least the experimental results for fullerenes in [32] can alternatively also be explained with the aid of MO-SFA-VG and thus within SAE [33]. Clearly, the validity of the SAE that in fact should depend on the molecular system and the laser-pulse parameters can only be judged on the basis of very accurate experimental data or full many-electron calculations. An advantage of the latter is that not only all possible ambiguities with respect to the spatiotemporal shape of the laser pulse can be removed, but it is also possible to separate purely electronic effects from the ones arising from orientation or vibrational motion. Therefore molecular hydrogen for which very accurate two-electron calculations can be performed [34–36] was chosen as a first test case for the newly developed SAE-TDSE code for molecules. It should be stressed, however, that SAE-TDSE is a general approach that can be applied even to large polyatomic systems.

After a description of the method in Sec. II the basis-set parameters and adopted density functionals used in the subsequent calculations are specified in Sec. III. The results are presented and discussed in Sec. IV followed by a conclusion and outlook in Sec. V. Atomic units are used, if not stated otherwise.

II. METHOD

A. SAE-TDSE

The nonrelativistic time-dependent Hamiltonian describing the electrons of a molecular system exposed to a laser pulse where the latter is treated classically can be written as

$$\hat{H}(t) = \hat{H}_{\mathrm{mol}} + \hat{H}_{\mathrm{int}}(t). \tag{1}$$

$\hat{H}_{\mathrm{mol}}$ is the time-independent Hamiltonian describing the electronic motion of the molecular system while $\hat{H}_{\mathrm{int}}(t)$ represents the time-dependent laser-electron interaction. In the dipole approximation that is adopted here the interaction term may be expressed in the length or velocity gauge form. The wave functions obtained with either gauge differ only by a phase factor. Therefore all physical observables obtained with the two wave functions agree, if the wave functions are exact. In practice, the use of a finite representation for the wave function may lead to differences, if the results are not sufficiently converged. In turn, the convergence behavior is gauge dependent, since the finite basis has to represent the phase factor occurring in one gauge but absent in the other one. In the present work the velocity gauge is adopted that usually shows faster convergence properties [35,37]. The interaction term is then given by [1]

$$\hat{H}_{\mathrm{int}}(t) = -\frac{\mathbf{A}(t)\cdot\mathbf{P}}{c}, \tag{2}$$

where c is the vacuum speed of light, $\mathbf{A}(t)$ the time-dependent vector potential describing the laser pulse, and $\hat{\mathbf{P}}$ the momentum operator which is the sum over the momentum operators of the individual electrons.

In the SAE it is assumed that only a single electron responds to the laser field while all other electrons remain unaffected. In the usual interpretation of the SAE in the context of atoms or molecules exposed to strong fields this implies also that no relaxation due to a possible excitation or even ionization of the active electron is allowed for. Expressing

the many-electron wave function in the form of a single Slater determinant built by orthonormal one-electron wave functions ϕ_j that are eigenfunctions of $\hat{H}_{\mathrm{mol}}$, freezing all but one electron, and using orthonormality as well as Slater-Condon rules leads finally to an effective one-electron Hamiltonian,

$$\hat{h}(t) = \hat{h}_{\mathrm{mol}} + \hat{d}_{\mathrm{int}}(t). \tag{3}$$

The dipole interaction term $\hat{d}_{\mathrm{int}}(t)$ is equal to $\hat{H}_{\mathrm{int}}(t)$ in Eq. (2) but with the single-electron momentum operator $\hat{\mathbf{p}}$ instead of the total momentum operator $\hat{\mathbf{P}}$. The operator $\hat{h}_{\mathrm{mol}}$ describes the motion of the active electron in the potential formed by the nuclei and the remaining frozen electrons. For the single-determinant approximation this leads to the frozen Hartree-Fock, or static-exchange Hamiltonian $\hat{h}_{\mathrm{mol}}$. However, additional correlation effects can be formally included employing an appropriate optical potential. A simplified version is the use of a Kohn-Sham (KS) Hamiltonian

$$\hat{h}_{\mathrm{KS}}(\mathbf{r}) = -\frac{1}{2}\nabla_r^2 - \sum_{j=1}^{N} \frac{Z_j}{|\mathbf{r}-\mathbf{R}_j|} + \int \frac{n(\mathbf{r}')}{|\mathbf{r}-\mathbf{r}'|} d\mathbf{r}' + V_{\mathrm{xc}}[n(\mathbf{r})], \tag{4}$$

where N is the number of nuclei whose position vectors are $\mathbf{R}_j$, $n(\mathbf{r})$ is the ground-state electron density, and V_{xc} the exchange-correlation potential. (Note that the parametrical dependence of n and other quantities like the KS orbitals on the nuclear geometry is omitted here and in the following for reasons of better readability.)

The advantage of the KS Hamiltonian is that the numerically expensive calculation of the exchange integrals is avoided. This allows one in principle to treat large molecular systems and saves computational resources. A further important advantage compared to the HF Hamiltonian is the ability to include correlation into the calculation of the core. An evident disadvantage is the unknown exact functional. As is discussed below, the proper choice of a functional is important for the success of the present approach. Note there is no principle obstacle to use HF theory or a more elaborate many-body potential, at a cost of a more involved computational treatment. In fact, for the example of H_2 considered in this work, HF-based SAE calculations are performed for comparison. For this purpose, the static potential generated by a singly occupied Hartree-Fock orbital $\phi_{1\sigma_g}^{\mathrm{HF}}$ was employed for the calculation of the excited states. In this case $\hat{h}_{\mathrm{KS}}$ in Eq. (4) becomes equivalent to the Hartree-Fock Hamiltonian $\hat{h}_{\mathrm{HF}}$, if $n(\mathbf{r}) = |\phi_{1\sigma_g}^{\mathrm{HF}}(\mathbf{r})|^2$ and $V_{\mathrm{xc}}=0$ are used.

The evaluation of the KS orbitals that solve the eigenvalue problem

$$\hat{h}_{\mathrm{KS}}(\mathbf{r})\phi_i(\mathbf{r}) = \epsilon_i \phi_i(\mathbf{r}) \tag{5}$$

is performed in the two-step procedure described in detail in [38]. First, a conventional bound-state DFT calculation using the linear combination of atomic orbitals (LCAO) approach is performed using program ADF [39,40]. This program adopts Slater-type orbitals as basis functions. The obtained electron density $n(\mathbf{r})$ is then used to set up the matrix of the KS Hamiltonian (4) in an alternative set of basis functions that is more suitable for the present purpose.

These basis functions consist of a product of a symmetry-adapted linear combination of real spherical harmonics $[Y_{lm}^R(\theta,\phi)]$ and a radial B-spline function,

$$\chi_{n,l,h,\lambda,\mu}^s(\mathbf{r}) = \sum_{j\in Q_s} \frac{B_n^k(r_j)}{r_j} \sum_{m=-l}^{l} b_{l,m,h,\lambda,\mu,j} Y_{lm}^R(\theta_j,\varphi_j). \tag{6}$$

In Eq. (6) s is an index that is related to the center of the basis function which defines the origin of a local spherical coordinate system for $\mathbf{r}_j=\{r_j,\theta_j,\varphi_j\}$. The origin of the central coordinate system is denoted by $s=0$. It is usually chosen to agree with the center of charge of the molecule. In the spirit of the LCAO approach $s>0$ runs over the nonsymmetry equivalent nuclei and defines therefore atom-centered basis functions. The molecular symmetry is accounted for by the sum over j. It runs over the number Q_s of nuclei that are symmetry equivalent to nucleus s. The coefficients $b_{l,m,h,\lambda,\mu,j}$ are also determined by the molecular symmetry and provide symmetry-adapted linear combinations of the spherical harmonics. The indices λ, μ, and h specify the irreducible representation (IR), the subspecies in case of degenerate IRs, and an identifier in case of different elements with agreeing $\{l,\lambda,\mu\}$, respectively. Finally, B_n^k specifies the nth B spline of order k.

The radial B-spline functions are defined by a grid of knots and the interval $[0, r_{\mathrm{max}}^s]$ covered by the knot sequence. In the present implementation of the code the values of r_{max}^s for $s>0$ have to be chosen in such a way that the spheres defined by different values of $s>0$ do not overlap. Continuity of the second derivative over the surfaces of these spheres is achieved by removing the last three B-spline functions of each set. The set of central basis functions denoted by $s=0$ covers on the other hand a large sphere (with radius r_{max}^0) that includes all other spheres. In fact, for the present application, r_{max}^0 is chosen much larger, since its value determines the number of Rydberg states and the density of states in the electronic continuum that are obtained with a given basis set. The reason is that for a given value of r_{max}^0 the diagonalization of the KS Hamiltonian in the given basis yields only those states whose density is confined to a smaller volume or that (accidentally) happen to possess a node at r_{max}^0. Although it is possible to obtain alternatively any continuum state using the so-called free-boundary approach [38,41], the "box" discretization achieved by a fixed-boundary approach appears more suitable for the present purpose. The reason is that the discretized continuum obtained this way fulfills a number of sum rules and allows one therefore to substitute integrals over continuum states to be replaced by simple sums over their discretized counterparts.

Once the set of eigenfunctions ϕ of the field-free KS Hamiltonian (4) has been obtained, one of the orbitals that is occupied in the initial state can be selected as the active one. It is used together with all initially unoccupied orbitals as a basis for solving the time-dependent Schrödinger equation defined by the Hamiltonian in Eq. (3). Insertion of

$$\Psi(\mathbf{r},t) = \sum_{i,\lambda,\mu} c_{i,\lambda,\mu}(t)\phi_{i,\lambda,\mu}(\mathbf{r}) \tag{7}$$

into

$$i\frac{\partial\Psi(\mathbf{r},t)}{\partial t} = \hat{h}(t)\Psi(\mathbf{r},t) \tag{8}$$

and multiplication from the left with $\phi^*_{j,\kappa,\nu}(\mathbf{r})$ yields after integration over the electronic coordinates

$$i\frac{dc_{j,\kappa,\nu}(t)}{dt} = \epsilon_{j,\kappa,\nu}c_{j,\kappa,\nu}(t) + \sum_{i,\lambda,\mu} d_{j,\kappa,\nu;i,\lambda,\mu}c_{i,\lambda,\mu}(t). \tag{9}$$

In Eq. (9) the electronic dipole transition matrix elements $d_{j,\kappa,\nu;i,\lambda,\mu}=\langle\phi_{j,\kappa,\nu}|\hat{d}(t)|\phi_{i,\lambda,\mu}\rangle$ were introduced. Depending on the molecular symmetry different dipole-selection rules apply. This leads to various block structures of the coupled set of ordinary first-order differential equations (9). The time-dependent coefficients $c_{i,\lambda,\mu}$ are obtained numerically using a variable-order, variable-step Adams routine. The approach for solving the TDSE is thus very similar to the one implemented earlier for treating the full electronic problem of H_2 exposed to intense laser pulses described in [35] that is also used in the present work in order to obtain reference data. The only difference is that in the SAE-TDSE approach presented in this work an effective one-electron Hamiltonian is used together with KS orbitals while previously the full two-electron Hamiltonian was adopted using configuration interaction (CI) wave functions. In the resulting CI-TDSE approach Eq. (1) is solved [instead of Eq. (3)] by an expansion of the time-dependent two-electron wave function in terms of field-free CI wave functions describing H_2 in the fixed-nuclei approximation. This gives essentially exact results for the nonrelativistic electronic problem of H_2 exposed to a laser pulse within the dipole approximation.

B. MO-SFA

In view of the different implementations of MO-SFA, a brief description of the one adopted in this work is given. Following [42] the total SFA ionization rate within the SAE approximation [in the linear polarized harmonic laser field $\mathbf{F}(t)=\mathbf{F}\cos\omega t$ with period $T=2\pi/\omega$ and intensity I] can be expressed as the sum over N-photon processes

$$W = \sum_{N=N_{\min}}^{\infty} W_N,$$

$$W_N = \frac{p_N}{(2\pi)^2}\int d\hat{\mathbf{p}}|A(p_N\hat{\mathbf{p}})|^2, \tag{10}$$

where $p_N=\sqrt{2(N\omega-I_p-U_p)}$ with ionization potential I_p and ponderomotive energy $U_p=I/(2\omega)^2$. The minimum number of photons $N_{\min}$ is determined by energy conservation. Using the momentum wave function

$$\tilde{\phi}(\mathbf{p}) = \int d^3r e^{-i\mathbf{p}\cdot\mathbf{r}}\phi(\mathbf{r}) \tag{11}$$

of the active electron the transition amplitude $A(p_N\hat{\mathbf{p}})$ is given as

$$A(\mathbf{p}) = \frac{1}{T}\int_0^T dt\tilde{\phi}(\mathbf{q})\left[\frac{\mathbf{q}^2}{2}+I_p\right]e^{iS(t)}. \tag{12}$$

Here,

$$S(t) = \int_0^t dt'\left[I_p + \frac{1}{2}\boldsymbol{\pi}^2(t')\right] \tag{13}$$

is expressed via the mechanical momentum of the active electron, $\boldsymbol{\pi}(t)=\mathbf{p}-(\mathbf{F}/\omega)\sin\omega t$, and

$$\mathbf{q} = \begin{cases} \mathbf{p} & \text{V-gauge} \\ \boldsymbol{\pi}(t) & \text{L-gauge} \end{cases}. \tag{14}$$

It is possible to avoid the evaluation of the highly oscillatory integral in Eq. (12) by means of a transformation of the integration path into the complex plane [43,44]. Ionization yields are obtained from the rates by an integration over the pulse.

The ADF code provides the KS orbitals $\phi(\mathbf{r})$ as a linear combination of Slater-type orbitals (STO). In the case of a homonuclear diatomic molecule, symmetry allows one to rewrite the orbitals as

$$\phi(\mathbf{r}) = \sum_j C_j\varphi_j(\mathbf{r}) \tag{15}$$

with the molecular orbitals $\varphi_j(\mathbf{r})$ expressed in terms of the one-center STOs as

$$\varphi_j(\mathbf{r}) = \psi_j(\mathbf{r}+\mathbf{R}/2) + s_j\psi_j(\mathbf{r}-\mathbf{R}/2), \tag{16}$$

where $|s_j|=1$. The Fourier transform of $\phi(\mathbf{r})$ is thus given as

$$\tilde{\phi}(\mathbf{p}) = \sum_j 2C_j \times \begin{Bmatrix} i\sin(\mathbf{p}\cdot\mathbf{R}/2), & s_j=-1 \\ \cos(\mathbf{p}\cdot\mathbf{R}/2), & s_j=1 \end{Bmatrix} \times \tilde{\psi}_j(\mathbf{p}), \tag{17}$$

where $\tilde{\psi}_j(\mathbf{p})$ are the Fourier-transformed STO basis functions

$$\tilde{\psi}_j(\mathbf{p}) = \int d\mathbf{r}e^{-i\mathbf{p}\cdot\mathbf{r}}\psi_j(\mathbf{r}). \tag{18}$$

A simplified expression can be obtained [42] if the orbital $\phi(\mathbf{r})$ is for sufficiently large values of r approximated by

$$\phi(\mathbf{r}) \approx \sum_l C_l r^{\nu-1}e^{-\kappa r}Y_{l0}(\hat{\mathbf{r}}), \tag{19}$$

with $\nu=Z/\kappa$ and $\kappa=\sqrt{2I_p}$. The onset of the validity of this approximation that is also the basis for MO-ADK may be denoted by the parameter r_{as}. Use of Eq. (19) leads in the vicinity of $\pm i\kappa$ to

$$\tilde{\phi}(\mathbf{p}) \approx \sum_l C_l\frac{4\pi(\pm1)^l(2\kappa)^\nu\Gamma(\nu+1)}{(p^2+\kappa^2)^{\nu+1}}Y_{l0}(\hat{\mathbf{p}}), \tag{20}$$

where $|p\mp i\kappa|<r_{\text{as}}^{-1}$ should be fulfilled. Since a significant contribution to the transition amplitude arises from the range

$$|p\mp i\kappa| < \sqrt{\omega}(1+\gamma^{-2})^{1/4} \tag{21}$$

with the Keldysh parameter $\gamma=\sqrt{I_p/(2U_p)}$, the restriction

$$\omega\sqrt{1+\gamma^{-2}} < r_{\mathrm{as}}^{-2} \tag{22}$$

can be obtained as an estimate for the validity of the simplified approach based on Eq. (20).

While the original formulation of SFA is based on complete neglect of the interaction of the remaining ion on the active electron, once it is ejected, there have been proposals to incorporate this neglected Coulomb interaction at least in some approximate way. An empirical Coulomb-correction factor $C_{\mathrm{BC}}^2=(\kappa^3/F)^{2Z/\kappa}$ was proposed for the atomic SFA rate in velocity gauge in [45] and later on also used for molecules. Here, F is the electric field strength. As is discussed in [44], this Coulomb-correction factor is for 800 nm and the hydrogen atom close to a factor that can be obtained by postulating the MO-SFA-VG rate to converge for laser frequency $\omega\rightarrow 0$ to the known tunneling result. Considering that $\phi(\mathbf{r})$ of H_2 is essentially spherical, one may use the result obtained for the $1S$ state of a hydrogenlike atom, but substituting n with ν. Using $\nu\approx 1$ to simplify the coefficients, a simplified version of the Coulomb-correction factor proposed in [44] reads for H_2

$$C_{\mathrm{VC}}^2 = \frac{2}{\omega}\sqrt{\frac{3}{\pi}\frac{F^3}{\kappa^5}}\left(\frac{\kappa^3}{F}\right)^{2\nu}. \tag{23}$$

Note that for the laser parameters discussed in this work the Coulomb-correction factors C_{BC}^2 or C_{VC}^2 often even exceeds a factor of 100 and have thus a very large impact on quantitative predictions.

In [18] it was concluded that MO-SFA-LG gave better agreement to experimental data, if no Coulomb correction is used. Therefore in that and subsequent works by those authors MO-SFA-LG results were presented without any Coulomb correction. The prescription of omission of any Coulomb factor was consequently followed also in the present work.

III. COMPUTATIONAL DETAILS

Besides the limitations intrinsic to the SAE the correctness of the present numerical approach is influenced by the quality of the basis set and the chosen potential V_{xc}. While the basis-set dependence can be systematically investigated by a variation of the basis-set parameters, the choice of V_{xc} incorporates an unknown systematic error. In the present work the influence of both the basis set as well as the one of V_{xc} was investigated.

The question of basis-set quality may be further split by considering two different issues. One is the description of the molecular ground-state properties, the other is its ability to properly describe the time-dependent wave function of the active electron in the combined potential of the remaining electrons and the laser field. The description of the molecular ground-state properties and thus the quality of the KS Hamiltonian (4) is determined by the STO basis used in the ADF program run and the completeness especially of the nuclei-centered B-spline basis functions ($\chi_{n,l,h,\lambda,\mu}^{s}$ with $s\neq 0$). In the present work both DZP (two $1s$ and one $2p$ STO functions) and extended, even-tempered ET (four $1s$, two $2p$, and one $3d$ STO functions) basis sets were tested. All results agreed within the graphical resolution of the figures shown in this work.

The main basis-set parameters responsible for an adequate description of the active electron itself are the radius r_{max}^0 of the central sphere in which the radial basis is confined, the number of B splines, and the number of angular momenta l specified by l_{max}. Since a linear grid sequence was used for the knot points, the number of B splines fixes together with r_{max}^0 the spacing Δr between the knots. A further parameter is the order k of the B splines. However, an increase of the order allows only to achieve a similar result with a sparser knot sequence. Therefore the investigation of convergence with respect to either number of B splines or their order is somehow redundant in the sense that if convergence is achieved with respect to one parameter, it should also be obtained with respect to the other. It is often practical to introduce an energy cutoff ϵ_{cut} as a further parameter. In this case only those KS orbitals are included in the expansion (7) of the time-dependent wave function Ψ that possess an energy smaller than ϵ_{cut}.

It was found that converged excitation and ionization yields were obtained for the investigated ranges of laser parameters when choosing $r_{\mathrm{max}}^0 \geq 120\ a_0$ with a linear spacing of the knot sequence $\Delta r \leq 0.65\ a_0$. This was confirmed by performing calculations varying r_{max}^0 in between 120 and 240 a_0 and by a variation of Δr between 0.70 and 0.40 a_0. A variation of the highest angular momentum l_{max} between 10 and 16 revealed no visible differences. Convergence with respect to ϵ_{cut} was investigated by a variation of this parameter in steps of 10 a.u. in between 10 and 40 a.u. Good convergence was found. All shown results were obtained with $\epsilon_{\mathrm{cut}}=40$ a.u.

In addition to the simple Hartree (static) potential generated by the Hartree-Fock $1\sigma_g$ orbital of H_2, a number of DFT V_{xc} potentials were tested in order to investigate the sensitivity of the results on the chosen functional. The ground-state local-density approximation LDA [46] using the VWN functional [47], the transition-state LDA (TSLDA) with a half electron removed that gives much better transition energies, and the van Leeuwen–Baerends 1994 (LB94) functional [48] have been employed. TSLDA consists in the application of Slater's transition-state technique to the LDA functional [49]. The LB94 functional ensures the correct Coulombic-asymptotic behavior and gives better results for polarizabilities as well as single photon excitation and photoionization spectra [50].

Molecular hydrogen was chosen as a first test case of the SAE-TDSE approach, since it is possible to compare with full two-electron calculations. As described in detail in [35] the two-electron code solves the TDSE in a basis of field-free states, too. The latter are, however, now fully correlated solutions of the complete two-electron Hamiltonian. The field-free wave functions are obtained from a CI calculation performed in the basis of orbitals that are solutions of the one-electron Hamiltonian in which the electron-electron interaction is completely neglected. The orbitals are expressed in prolate spheroidal coordinates ($1\leq\xi<\infty$, $-1\leq\eta\leq 1$, $0\leq\varphi<2\pi$) and expanded in products of B splines along the two radial coordinates, while the angular part is simply given by the cylindrical symmetry and thus by the

TABLE I. Ionization potentials (I_p) and (where applicable) $C_l \equiv C_{l,m=0}$ coefficients for H_2 ($R=1.4$ a_0) obtained with different electronic structure calculations. This includes the density-functional approaches using the LB94 or the TSLDA functionals as well as the Hartree-Fock (HF), $X\alpha$, or configuration-interaction (CI) method.

Method	I_p (eV)	C_0	C_2	C_4
HF	16.188	2.435	0.1073	0.0010
HF [6]	16.449	2.44	0.14	
$X\alpha$ [17]	15.70	2.51	0.06	0.00
LB94	15.32	1.146	0.0666	0.0008
TSLDA	17.40	0.4521	0.0231	0.0002
LDA	10.26			
SAE-CI	15.49			
CI	16.06			

exponential functions $\exp(im\varphi)$. Details concerning the used CI method can be found in [51]. The orbitals were obtained with 350 B splines of order 15 in the ξ direction (covering $1 \leq \xi \leq 350$ a_0) and 24 B splines of order 8 along η. H_2^+ orbitals obtained with this basis with angular momenta $0 \leq m \leq 5$ were used to build configurations for the CI calculation of the H_2 states with either $^1\Sigma_g$ or $^1\Sigma_u$ symmetry. About 6000 (5800) configurations were used in the CI calculations for $^1\Sigma_g$ ($^1\Sigma_u$). The same energy cutoff $\epsilon_{\text{cut}} = 40$ a.u. used for SAE-TDSE was also adopted in the CI-TDSE calculations.

As in a previous work [35] also a pseudo-SAE calculation is performed. In this case only configurations with one of the electrons occupying the lowest lying σ_g orbital of H_2^+ are included in the CI calculation. Using the same orbitals as for the full CI calculation, this leads to about 4200 configurations for $^1\Sigma_g$ and $^1\Sigma_u$ symmetry. This approach is called SAE-CI in the following.

In Table I the vertical ionization potentials I_p (at the equilibrium distance $R=1.40$ a_0 at which all calculations in this work were performed) obtained with the different DFT functionals, the Hartree-Fock potential, and the two CI calculations (full and SAE-CI) are listed. In order to calculate MO-ADK rates one needs also the so called $C_{l,m}$ coefficients [17]. In the present case of H_2 only the values for $m=0$ are required and given for the independent-particle models DFT and HF. For comparison, also some literature values used previously for MO-ADK and MO-SFA-LG calculations are given. While the HF parameters found in the present approach are quite similar to the ones found with the aid of a numerical HF program [6], the DFT results differ more evidently. They are not only deviating from the HF results, but also among each other. Of course, it should be kept in mind that it is a rather well-known fact that few-electron atoms and molecules like He and H_2 are notoriously difficult tasks for DFT. No C_l coefficients are given for LDA, since the asymptotic behavior of the HOMO obtained with this functional differs too much from the correct one. Therefore no senseful fit could be performed for the determination of the C_l coefficients.

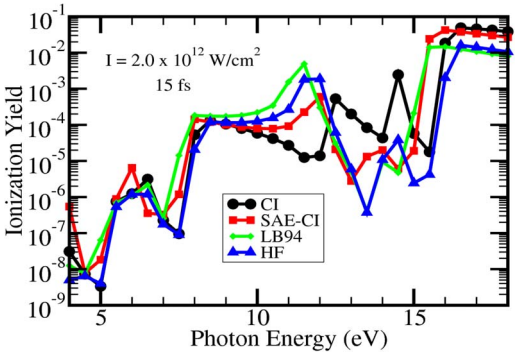

FIG. 1. (Color online) Ionization yield of H_2 (at $R=1.40$ a_0) as a function of the photon energy for a linear polarized laser with a parallel orientation of polarization vector and molecular axis, a peak intensity of 2.0×10^{12} W/cm^2, and full pulse duration of 15 fs. The results obtained with the SAE-TDSE approach using either the LB94 functional (green diamonds) or HF functional (blue triangles) are compared to a pseudo-SAE model (SAE-CI, red squares) and to a full two-electron CI (black circles) calculation.

In all calculations in this work a linear polarized laser pulse with the polarization vector parallel to the molecular axis is used. The amplitude of its vector potential along the molecular axis is given by

$$A(t) = \frac{E_0}{\omega}\cos^2\left(\frac{\pi t}{T}\right)\cos(\omega t), \tag{24}$$

where E_0 is the peak electric field strength, ω the central carrier frequency, and T the pulse duration, since a single pulse is defined in the time interval between $-T/2$ and $T/2$. As is discussed in [37], the advantage of such a pulse shape is the well-defined integration time due to the sharply defined pulse duration. In the case of a usually more realistic Gaussian pulse shape (that is among other ones also incorporated in our code) the less well-defined pulse duration makes the time integration more demanding, since for every time propagation convergence with respect to the time limits has to be checked.

IV. RESULTS

A. Photon-frequency variation

Figure 1 shows the photon-frequency dependence of the ionization yield of H_2 for a 15 fs laser pulse and a peak intensity of 2×10^{12} W cm^2. For this laser intensity and the shown photon frequencies the molecular response is still almost perturbative [35]. The displayed frequency range covers parts of the 1–4-photon regime. While the overall behavior agrees for all the adopted SAE models as well as for the full CI calculation, there are pronounced differences. These are due to the different excitation energies and ionization potentials I_p. The low I_p values obtained with the LB94 functional and the pseudo-SAE-CI leads to a shift of the N-photon thresholds to lower photon energies compared to the values found for the HF and the full CI calculation. As was demonstrated in [35] it is approximately possible to correct for the different I_p values by a corresponding rescaling of the photon frequency.

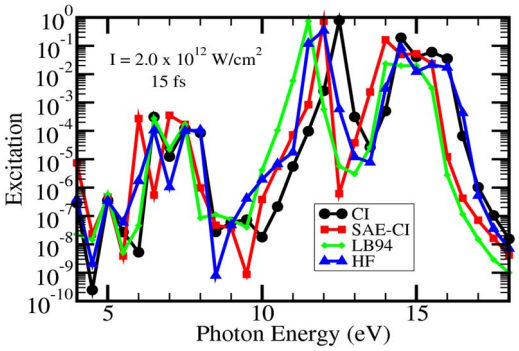

FIG. 2. (Color online) As Fig. 1, but showing the excitation to all electronic excited bound states.

The pronounced structure found in the two-photon regime between about 7.5–8 and 15–16 eV is due to resonance-enhanced multiphoton ionization (REMPI), especially through the $B\ ^1\Sigma_u$ and the $B'\ ^1\Sigma_u$ states. Since the SAE models underestimate the excitation energies to these states, the REMPI peaks are shifted to smaller photon energies. The only exception is the $B'\ ^1\Sigma_u$ state obtained with the HF approach whose position agrees quite well with the CI result. In general the HF results are closer to the full CI results, since also the ionization potentials agree better.

Figure 2 shows the excitation yield for the same laser parameters used in Fig. 1. The excitation yield is defined as the population left in all electronic states except the one of the initial ground state as well as the total population of the electronic continuum. Besides the resonant population of the $B\ ^1\Sigma_u$ state at about 12 to 13 eV one notices a rather large excitation not only at the energy of the $B'\ ^1\Sigma_u$ state but also for slightly larger photon energies until the one-photon ionization threshold. This is due to a large resonant population of Rydberg states. Similar effects are also seen at the two-, three-, and four-photon thresholds.

In view of the rather pronounced frequency dependence of the ionization and excitation yields (note the logarithmic scale) it is clear that a calculation for a fixed photon frequency that does not take into account the error in the ionization and excitation energies can easily give a completely wrong result. This problem should reduce if the nonperturbative multiphoton regime with higher laser intensities and smaller photon frequencies is considered. A typical case of interest in this regime is provided by laser pulses with a wavelength of 800 nm (corresponding to photon energy of about 1.55 eV). In the case of H_2 at $R=1.40\ a_0$ 10 to 12 photons are needed for reaching into the ionization continuum, depending on the adopted electronic structure model as can be seen from Table I.

B. Intensity variation

Figure 3 shows the dependence of the ionization yield on the peak intensity of a laser pulse with a central photon energy of 1.55 eV and 12 cycles duration (corresponding to about 32 fs). For comparison, the results obtained from the full two-electron CI calculation are compared to the ones from the SAE using different potentials to describe the frozen core. Also the results from the SAE-CI model are plotted. Clearly, the DFT functionals LDA and TSLDA give results that differ substantially from the correct two-electron yield. While LDA overestimates the yield (for a peak intensity of 10^{13} W cm^{-2} by more than two orders of magnitude), TSLDA underestimates the yield by a similar order of magnitude. In addition, the slope of the curves differs. The LB94 functional that imposes a correct asymptotic long-range behavior leads on the other hand to a much better agreement with the CI results. For peak intensities larger than 3×10^{14} W cm^{-2} the agreement is (on the logarithmic scale) very satisfactory. The Hartree-Fock potential leads to a very similar result and in fact the two SAE results with the HF or LB94 functional are aside from tiny local oscillations at lower peak intensities almost indistinguishable. In view of the rather different ionization potentials obtained for HF and LB94 functionals this result is quite remarkable, since for high intensities and long wavelengths (quasistatic regime) one usually expects the ionization yield to be mainly dependent on the ionization potential. In the spirit of a multiphoton picture one may point out that within the LB94 description ten photons are sufficient for ionization, while the HF potential requires 11 photons. A further surprise is the pronounced failure of the SAE-CI model in a large intensity range. For peak intensities between 10^{13} and 10^{14} W cm^{-2} the SAE-CI model agrees surprisingly well with the LDA result. For large peak intensities (and close to saturation for the given laser pulse) SAE-CI and LDA disagree, the SAE-CI result being then much closer to the full CI result.

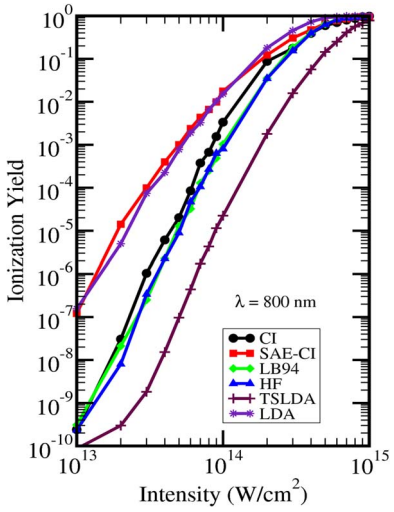

FIG. 3. (Color online) Ionization yield of H_2 (at $R=1.4\ a_0$) as a function of the laser peak intensity for a 800 nm (1.55 eV) laser pulse (linear polarization parallel to the molecular axis) with 12 cycles (about 32 fs) duration. Shown are the results obtained for full CI (black circles), SAE-CI (red squares), and the SAE-TDSE calculations using HF (blue triangles), LB94 (green diamonds), LDA (violet stars), and TSLDA (maroon crosses) functionals.

An intrinsic problem of the SAE is the question how equivalent electrons should be treated. In the present example of H_2 there are evidently two equivalent electrons that could be ionized (within the SAE model) independently of each other. Therefore it appears natural to scale the SAE

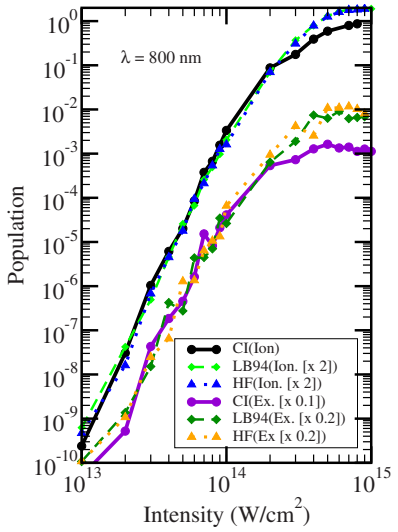

FIG. 4. (Color online) Ionization and excitation yields of H_2 for the same laser parameters as in Fig. 3. The ionization yields obtained with the SAE-TDSE calculations using HF (blue triangles) and LB94 (light green diamonds) functionals are scaled by a factor of 2 in an attempt to compensate for the two equivalent electrons when comparing to CI (black circles). Also shown are the excitation yields of CI (purple circles), HF (orange triangles), and LB94 (dark green diamonds) functionals, all scaled by a factor of 0.1 for better readability and the SAE-TDSE results (HF and LB94) by an additional factor of 2 for the two equivalent electrons.

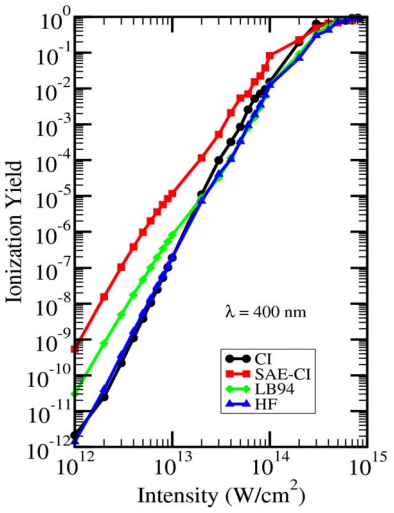

FIG. 5. (Color online) As Fig. 3, but for 400 nm (3.1 eV) laser wavelength, full pulse duration of 24 cycles (about 32 fs), and omitting the results for LDA and TSLDA.

yields by a factor of 2. The result is shown in Fig. 4 for the two SAE models HF and LB94 that gave reasonable agreement with the full CI result. Inclusion of the factor of 2 results indeed in a very good agreement of the SAE and the CI results for laser peak intensities up to about 2×10^{14} W cm^{-2}. At higher intensities the factor of 2 leads to an overestimation of the yield by the SAE model. This is expected from the good agreement found for intensities larger than 3×10^{14} W cm^{-2} without a factor of 2 in Fig. 3. On physical grounds it is also expected that a factor of 2 should not be appropriate for arbitrarily high intensities (or long laser pulses). If substantial ionization occurs, the remaining electron will see a less screened nuclear potential than before. Consequently, its ionization potential increases which, however, is not taken into account in the SAE approximation when adopting simply a factor of 2 for the yield. From Figs. 3 and 4 one can conclude that at least for H_2 and 800 nm wavelength the SAE results should be multiplied with a factor of 2 for ionization yields below 10%. This is qualitatively understandable, since the change of the screening due to ionization should be small, if the ionization yield is small. The agreement of the unscaled SAE with CI for ionization yields above about 20% appears on the other hand to be not easily explainable and may be an accidental coincidence.

Figure 4 shows in addition the total excitation yield defined as the population of all electronically excited bound states. The overall agreement between the shown SAE models and the full CI calculation is again reasonably good, but especially for higher peak intensities (close to saturation) there is a clear deviation that increases with increasing laser intensity. The agreement of LB94 and HF functionals is on the other hand in the whole intensity range satisfactory. In view of the different excitation energies obtained with the two core potentials the agreement confirms that for H_2, 800 nm radiation, and the considered intensities the molecular response may be more ascribed to quasistatic- than to multiphoton-like behavior. This is further confirmed by the fact that neither the ionization nor the excitation curve shows pronounced signatures of REMPI or intensity-dependent channel closings.

Figure 5 shows the ionization yield for a 400 nm wavelength (corresponding to the second harmonic of 800 nm) obtained with either the CI or different SAE models. In order to maintain the same pulse duration as for 800 nm, the number of laser cycles is doubled. The agreement of SAE-HF and CI is again quite satisfactory, but not as good as for 800 nm. The main reason for the deviation is a channel closing occurring in the HF calculation at an intensity close to 2×10^{13} W cm^{-2} which is absent at this intensity in the CI result. This leads to an accidental very good agreement between the unscaled HF and the CI result which is reduced, if the HF yield is multiplied by a factor of 2 to account for the two equivalent electrons.

The intensity at which a channel closing occurs should depend (for a given laser pulse and thus ponderomotive energy) on the ionization potential. Although this simple argument may explain why the channel closing visible at 2×10^{13} W cm^{-2} cannot be seen in the CI yield, the same argument would predict a completely different channel-closing intensity for the LB94 result, since the ionization potentials of the HF and the LB94 functionals differ more than the ones of the HF and the CI calculation. On the contrary, the channel closing occurs at almost the same intensity for the HF and LB94 functionals, but its consequences are only more pronounced for the LB94 functional. This leads to the observed deviation between LB94 and HF functionals for intensities below 2×10^{13} W cm^{-2}. For higher intensities the yields predicted in these two SAE models agree on the other hand very well.

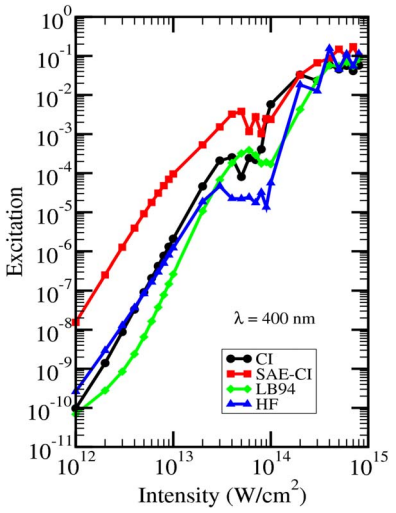

FIG. 6. (Color online) As Fig. 5, but showing the excitation yield.

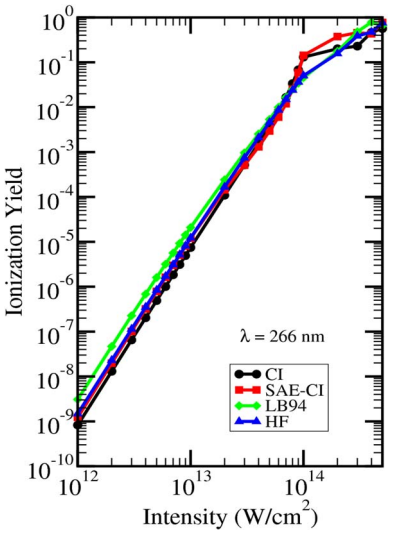

FIG. 7. (Color online) As Fig. 5, but for 266 nm (4.65 eV) and 36 cycles (about 32 fs).

A possible explanation for the good agreement of the channel-closing intensity for HF and LB94 functionals may be the fact that its value depends not only on the ponderomotive energy that has to be added to the ejected electron in order to be ionized in the presence of a laser field. The real ionization potential in a laser field is given by the energy difference between the final state (ion and ionized electron with zero momentum) and the initial state (neutral molecule). Therefore the ac Stark shift (laser-field dressing) of the initial ground state of the neutral molecule has to be considered in a determination of the ionization potential in a laser field and thus for the question at which intensity the number of photons necessary for reaching the ionization threshold increases or decreases. In view of the already discussed good agreement between the LB94 and HF functionals' yields for 800 nm (and at higher intensities for 400 nm), in the quasistatic regime it appears that the difference in the field-free ionization potentials is largely compensated by the ac Stark shifts of the neutral ground state.

From the three shown SAE models it is again the SAE-CI approach that gives the poorest agreement with the CI yields to which it agrees best at the highest intensities. It is also remarkable that the shape of the curve follows very closely the LB94 result to which it runs (on the logarithmic scale) almost parallel for intensities below about 10^{14} W cm^{-2}. The absolute difference is, however, about one order of magnitude. The SAE-CI model overestimates also the excitation yield, as can be seen from Fig. 6. At 400 nm the intensity-dependent excitation yields contain much more structure than for 800 nm, in agreement with the fact that for this wavelength the molecular response should be more multiphotonlike. The overall best agreement with the CI result is obtained with the HF functional, but the LB94 functional still works reasonably well and actually yields better agreement with CI than the HF functional in the intensity range between about 3×10^{13} and 8×10^{13} W cm^{-2}. Below these intensities the LB94 functional underestimates the excitation yield. The agreement of the HF functional to CI is on the other hand partly due to the different slopes of the two curves which leads to a crossing and thus to an accidental perfect agreement at about 4×10^{12} W cm^{-2}.

For a wavelength of 266 nm (third harmonic of 800 nm) the overall agreement between the ionization yields predicted by the SAE models and full CI is good, as can be seen in Fig. 7. In this case also the SAE-CI works very well, in fact it yields the best results. HF and LB94 functionals agree very well with each other above about 4×10^{13} W cm^{-2}. Below this intensity the LB94 functional yield is larger than the one obtained with HF. Since already the HF functional overestimates the yield slightly, the LB94 functional deviates from the CI result even more than the HF functional for these intensities. Above 10^{14} W cm^{-2} the agreement of the HF and LB94 functionals with the full CI calculation is not so good, since the CI yield shows some structure that is absent in the HF and LB94 functionals, but also present in the SAE-CI yield, though the quantitative agreement with the full CI result is not at all perfect. The overall rather satisfactory agreement between the CI and the SAE models at this rather short wavelength may appear surprising on the first glance, since one usually expects the structure to become more important as the wavelength decreases. However, it has to be reminded that for this photon energy of 4.65 eV one finds that four photons are required for reaching the ionization threshold for all shown models, since the ionization potentials vary only between 15.32 (LB94) and 16.19 eV (HF). Furthermore, the ponderomotive shift is inverse proportional to λ^2 and thus quite small for $\lambda=266$ nm compared to $\lambda=400$ or even 800 nm. On the other hand it is worth emphasizing that the good agreement between SAE and CI is in fact not as good, if one reminds that according to the discussion above the SAE results should be multiplied by a factor of 2 in order to account for the two equivalent electrons. Since the SAE yields are already without this factor slightly larger than the CI results, a factor of 2 will increase the difference.

The importance of the details of the electronic structure at this wavelength becomes on the other hand clearly evident, if the excitation yield shown in Fig. 8 is considered. The dif-

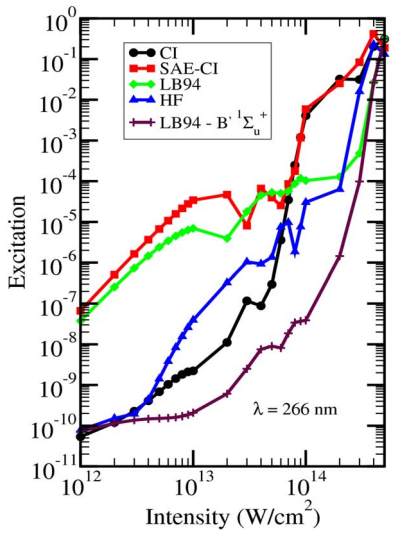

FIG. 8. (Color online) As Fig. 7, but showing the excitation yield. The additional curve (maroon crosses) is the excitation yield obtained with the LB94 functional, but omitting the contribution of the at this wavelength resonant $B'\ ^1\Sigma_u^+$ state.

ferent models predict very different excitation yields that can vary by many orders of magnitude. Also the intensity dependence and thus the slope of the curves differ dramatically between the different models. The best overall agreement with the CI result is found for HF. However, for intensities above 8×10^{13} W cm^{-2} the agreement between CI and SAE-CI is very good and much better than any agreement found between CI and the two other SAE models. It is interesting to note that, for example, at 10^{13} W cm SAE-CI predicts a larger excitation than ionization yield, while the full CI calculation gives an excitation yield that is orders of magnitude smaller than the one of ionization. Nevertheless, the absolute ionization yield predicted by the two models agrees very well at this intensity (Fig. 7). As was discussed in Sec. IV A, for short wavelengths the results of different models can differ dramatically due to the difference in excitation energy and thus position of intermediate resonances. The largely overestimated excitation yield of the LB94 functional at 266 nm is due to the fact that within this model the B' state is in three-photon resonance. This is immediately apparent if the excitation yield excluding the population of the B' state is plotted. The excitation yield drops by orders of magnitude and agrees at low intensities well with the HF and the CI predictions. The overestimation of the ion yield found for the LB94 model compared to the HF model is also a consequence of this REMPI process. Since the relative importance of REMPI, i.e., the enhancement of the ionization yield due to intermediate resonances, decreases with increasing intensity the better agreement of the HF and LB94 ionization yields for high intensities is understandable.

C. Comparison to simplified SAE models

There are two main motivations for the present SAE approach. First, for large systems with many electrons full calculations of their behavior in strong laser pulses appears hopeless with the present computational resources. An SAE approach is the first step in the direction of few-electron models to such large systems. Second, it is possible to investigate the validity of strong-field models that adopt the SAE together with additional approximations. The most prominent examples are MO-SFA [2] and MO-ADK [17] to which a comparison is made in this work.

In a purely theoretical validation of those models it is possible to avoid the need for an averaging over a number of parameters. A comparison to experiment usually requires on the other hand averages to be performed over molecular parameters (rotational and vibrational degree of freedom and thus orientation and nuclear geometry, respectively) as well as over laser parameters like the spatiotemporal pulse profile. Furthermore, the parameters of intense laser pulses like pulse shape and peak intensity are often only known with limited precision. In view of the exponential dependence of the ionization yield on the laser intensity, an experimental uncertainty of 20% or more with respect to the peak intensity which is rather common in strong-field experiments makes quantitative comparisons difficult. As a consequence, these averagings and uncertainties can severely bias the conclusions of a comparison between theory and experiment. Finally, experiments are usually not obtaining absolute ionization yields and allow therefore only qualitative comparisons.

In the context of suppressed ionization the predictions of MO-ADK, MO-SFA-LG, and MO-SFA-VG were compared to experimental data for a number of diatomic molecules [18]. In that work it was found that MO-SFA-LG gives the overall best agreement with experiment. However, it was also concluded that the experimental data are insufficient for a clear answer. Another example for the insufficiency of experimental data to answer which gauge is more appropriate in SFA is the experimentally observed vibrational distribution in H_2^+ produced in the ionization of H_2 by strong laser fields [9]. The found non-Franck-Condon distribution was first predicted on the basis of an extended atomic ADK model that takes into account vibrational motion [7]. As was shown in [9] this model gives even good quantitative agreement. However, later on both MO-SFA-LG [10] and MO-SFA-VG [11] were also shown to give good agreement with the experimental data.

Another important aspect in the validation of SAE models is their dependence on the quality of the adopted electronic structure model (for example, HF vs DFT), including basis sets, etc. In the present work a consistent comparison is performed by using identical orbitals in SAE-TDSE, MO-ADK, MO-SFA-LG, and MO-SFA-VG. Since the electronic structure of H_2 is quite simple, one expects this aspect to become in fact even more important for more complicated molecular systems. Preliminary results obtained for larger molecules confirm this expectation.

1. Comparison to MO-ADK

MO-ADK is an extension of the atomic ADK model to molecules. In simple terms, this extension is achieved by fitting the long-range behavior of the molecular orbital asymptotically to hydrogeniclike orbitals. Since for the latter the ADK formula was derived, it is possible to obtain MO-

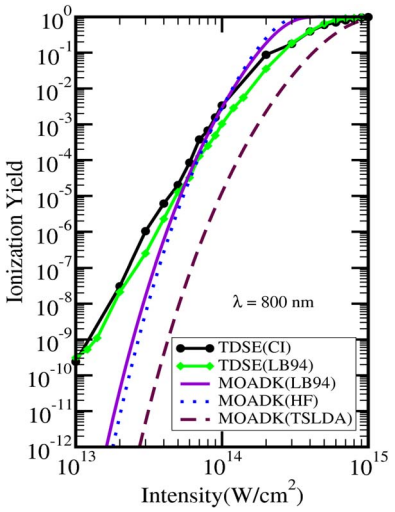

FIG. 9. (Color online) Ionization yield of H_2 for the same laser parameters as in Fig. 3. The results of CI-TDSE (black circles) and LB94 SAE-TDSE (green diamonds) functionals are compared to the MO-ADK prediction using the molecular parameters obtained with LB94 (purple solid), HF (blue dotted), and TSLDA (maroon dashes) functionals.

ADK rates from these fit coefficients, the so-called $C_{l,m}$. In the present case $m=0$ and the $C_l \equiv C_{l,m=0}$ are listed in Table I.

There are two practical problems related with the C_l coefficients. First, the asymptotic form to which the molecular orbital is fitted is only approximate. Second, the obtained coefficients depend quite strongly on the model and the numerical quality of the electronic-structure calculation with which the molecular orbitals are obtained, as is discussed in [18]. In [18] it was also found that this difference is even more pronounced for larger molecules than H_2. Nevertheless, as is evident from Table I, even for H_2 rather substantial differences between the C_l coefficients can be found. While the HF coefficients of this work compare reasonably well with the ones obtained from a numerical HF code used in [18], the LB94 coefficients differ by about a factor of 2. Note that in the present approach the long-range asymptotic tail of the highest occupied molecular orbital (HOMO) should be accurately described by the long-range *B*-spline expansion, so that the C_l coefficients extracted are expected to be numerically accurate.

The ionization yields obtained within the MO-ADK model by an integration of the rates over the corresponding laser pulses are shown for a laser wavelength of 800 nm in Fig. 9. Despite the very different ionization potentials and C_l coefficients there is rather good agreement between the HF and the LB94 MO-ADK ionization yields. Clearly, the difference in ionization potential is largely compensated for by the C_l coefficients. However, the slope obtained for the HF functional is slightly larger than the one of the LB94 functional. On the other hand, the use of the TSLDA functional for calculating the MO-ADK yield results in a much smaller value, in agreement with the higher ionization potential and thus not compensated for by the C_l coefficients. In fact, the *deviation* between the MO-ADK yields obtained with the LB94 functional or TSLDA is very similar to the one for the corresponding SAE-TDSE calculations (Fig. 3).

In Fig. 9 the predictions of the different MO-ADK models are also compared to the SAE-TDSE (LB94) and the full CI-TDSE results. [In view of the similarity of the SAE-TDSE ionization yields using either the LB94 or HF functional (Fig. 3) only the LB94 result is shown.] In the most favorable case, MO-ADK (LB94) should agree with SAE-TDSE (LB94). Every deviation is a clear indication of a failure of the MO-ADK model itself, since both calculations are based on the SAE and an identical description of the molecular structure. Clearly, MO-ADK predicts a wrong overall intensity dependence of the ion yield. Since the slope of the MO-ADK curve is too large but crosses the SAE-TDSE yield at a peak intensity of about 6×10^{13} W cm^{-2}, the predicted ion yield is too small at lower intensities and reaches too early saturation, i.e., complete single ionization. Only for intensities between 8×10^{13} and 1×10^{14} W cm^{-2} MO-ADK predicts the intensity dependence of the ionization yield in a qualitatively correct way, but overestimates it by about a factor of 2. This leads to an accidental agreement to the CI-TDSE result.

An analysis of the Keldysh parameter γ reveals that MO-ADK is in fact not really expected to work well even for 800 nm radiation. A condition for the applicability of a tunneling model is that the Keldysh parameter should be much smaller than 1. Within the HF or LB94 functional and at 800 nm γ is close to 1 at about 1×10^{14} W cm^{-2} which sets a lower limit to the applicability of MO-ADK. On the other hand, for intensities above about 2.5×10^{14} W cm^{-2} one reaches the classical over-the-barrier regime, i.e., the electron can escape over the field-suppressed potential barrier and ADK is known to overestimate the ionization rates. At this intensity γ has, however, only dropped to about 0.72. In the present example (H_2, 800 nm) qualitative agreement of MO-ADK with SAE-TDSE is found for γ close to or slightly larger than 1. For γ slightly smaller than 1 where ADK should be more appropriate the agreement is, however, worse. Therefore the found small range of qualitative agreement is shifted to slightly lower intensities than expected on the basis of the Keldysh argument.

In view of the fact that MO-ADK is expected to be valid only in a small intensity window for a laser wavelength of 800 nm, the value of the comparison shown in Fig. 9 may appear questionable, at least at first glance. However, the validity criterion is neither strict nor does it provide any information about the extent of a possible failure. The present work shows how MO-ADK fails both qualitatively and quantitatively for H_2 and the popular Ti:sapphire laser wavelength of 800 nm. Furthermore, the ADK model has often been used outside its range of validity to explain atomic or molecular behavior in intense laser fields. One example is the already mentioned suppressed ionization in molecules [13–16]. Noteworthy, MO-ADK was used to predict the occurrence or absence of suppressed ionization for a number of molecules in a correct way [17,18], although the adopted parameters would formally not allow one to apply ADK theory, since the Keldysh parameter was too large or the over-the-barrier ionization regime was reached. Another example is the observed lower saturation intensity of different charge states of fullerenes compared to the ADK predic-

tion and its attribution to a failure of the SAE in [31]. However, such an interpretation implicitly assumes ADK to correctly predict SAE yields.

In conclusion, Fig. 9 indicates that for H_2 and 800 nm MO-ADK fails even qualitatively to predict the overall intensity dependence of the ionization yield. Therefore MO-ADK can give in the best case only partially qualitatively correct predictions, while quantitative agreement occurs only accidentally. This is in agreement with an earlier work in which it was found that MO-ADK predicts the R dependence of the ionization rate of H_2 at 800 nm qualitatively correctly in the intensity range 10^{13} to 10^{14} W cm^{-2}, but its quantitative prediction is wrong [36]. As is clear from Fig. 9, the quantitative agreement at 10^{14} W cm^{-2} found in [36] is accidental, since it is due to a crossing and ignores the factor of 2 for the two equivalent electrons. Therefore claims based on quantitative arguments like, e.g., on a deviation between saturation intensities predicted by ADK and experimentally observed ones are problematic.

2. Comparison to MO-SFA

A second popular SAE-based approximation for predicting molecular ionization rates in intense laser fields is MO-SFA. Its validity regime is expected to be larger than the one of MO-ADK, but the calculation of the ionization rates is more demanding. This explains the popularity of ADK compared to SFA. While ADK is based on a length-gauge expression of the laser-matter coupling, SFA can—and was—formulated in velocity (MO-SFA-VG [2]) and in length (MO-SFA-LG [19]) gauge. Unfortunately, the results of SFA depend on the chosen gauge. Since SFA is a first-order approximation and thus a truncated series expansion of the correct scattering wave function, this gauge dependence is not surprising. On the other hand, it is clear that the two gauges cannot both give correct results, if the rates in the two gauges differ. From a practical point of view it is of great interest whether one of the gauges provides more reliable ionization rates than the other.

Figure 10 shows a comparison of the SAE-TDSE ionization yields as a function of intensity for the three wavelengths 800, 400, and 266 nm with the predictions of MO-SFA in velocity or length gauge. Two curves are shown for each of the two gauges. The velocity-gauge yields obtained with the Coulomb-correction factor of either Becker *et al.* (BC) or Vanne and Saenz (VC) are given. The two length-gauge curves correspond to either the full calculation using the molecular orbitals (STO) or to the approximate results obtained from the asymptotic fit coefficients C_l (C_{lm}).

The quantitative agreement between MO-SFA-VG(BC) and SAE-TDSE at 800 nm when using the HF approximation is almost perfect, at least on a double-logarithmic scale, as can be seen in Fig. 10(a). As was discussed before, the Coulomb-correction factor is essential for this quantitative agreement, since otherwise the yield predicted by MO-SFA-VG would be much too small. The MO-SFA-VG(VC) results agree with the SAE-TDSE data for high intensities, but underestimate the yield for lower intensities. The agreement of MO-SFA-VG(VC) with SAE-TDSE is, however, still better than the one found for MO-SFA-LG (without Coulomb correction). The latter underestimates the yield in the whole intensity range shown, but agrees with MO-SFA-VG(VC) for low intensities. The simplified MO-SFA-LG using the C_l coefficients works at 800 nm only for very high intensities, but leads otherwise to a further underestimation.

For $\lambda = 400$ nm [Fig. 10(b)] a very similar result is found. The best overall agreement with SAE-TDSE is achieved by MO-SFA-VG(BC), followed by MO-SFA-VG(VC), MO-SFA-LG(STO), and MO-SFA-LG (C_l). The deviation between the latter two is smaller than for 800 nm and thus the simplified approach based on the asymptotic form works better for 400 than for 800 nm. A closer look reveals, however, that despite the good overall quantitative agreement of MO-SFA-VG(BC) for lower intensities the predicted slope is slightly too small. The slopes predicted by the other MO-SFA approaches agree better to the one of SAE-TDSE. Also at very high intensities and thus close to saturation MO-SFA-VG(VC) works slightly better than MO-SFA-VG(BC).

For the lowest wavelength considered in this work, 266 nm [Fig. 10(c)], the failure of MO-SFA-VG(BC) to predict the correct slope is even more pronounced and occurs for the whole intensity range. As a consequence, it is now the MO-SFA-VG(VC) yield that shows the best overall agreement to SAE-TDSE, although its absolute value is still too small, except close to saturation. The MO-SFA-LG results possess a shape that is very similar to the one of MO-SFA-VG(VC), but the total yield is even smaller and deviates thus even more from SAE-TDSE. At 266 nm and for intensities below about 10^{13} W cm^{-2} one may in fact expect almost perturbative behavior, and the slope of the SAE-TDSE intensity curve in that regime is 3.94. This is very close to 4.0 which is the expected slope in lowest-order perturbation theory, since four photons of 4.65 eV are needed to reach the ionization threshold. Notably, this slope is rather constant for most of the intensity regime, except close to saturation, i.e., for an ionization yield larger than about 10%. MO-SFA-VG(BC) yields on the other hand a slope of 3.06. As is evident from the MO-SFA-VG(VC) and MO-SFA-LG results, this wrong slope is not a failure of SFA itself, but a problem of the Coulomb correction factor proposed by Becker *et al.* The deviation between SAE-TDSE and the different MO-SFA variants found for intensities larger than 10^{14} W cm^{-2} is of course not unexpected in view of the pronounced excitation at these laser parameters (see Fig. 8) and the fact that SFA (like ADK) does not consider excitation at all.

While the overall trends discussed so far for the HF results presented in Figs. 10(a)–10(c) appear to be reproduced by the DFT-LB94 results shown in Figs. 10(d)–10(f), there are some important and somewhat surprising differences. Although the HF and LB94 SAE-TDSE results for 800 nm agreed very well (Fig. 3), there is an evident deviation between MO-SFA-VG(BC) and SAE-TDSE when using the LB94 functional [Fig. 10(d)], despite the perfect agreement found for the HF approximation [Fig. 10(a)]. In fact, if the LB94 functional is employed in the SFA calculation, it is now MO-SFA-VG(VC) that yields a very good agreement (except at very low and very high intensities) with SAE-TDSE. MO-SFA-LG(STO) yields also rather good results, but clearly not as good as MO-SFA-VG(VC) and slightly

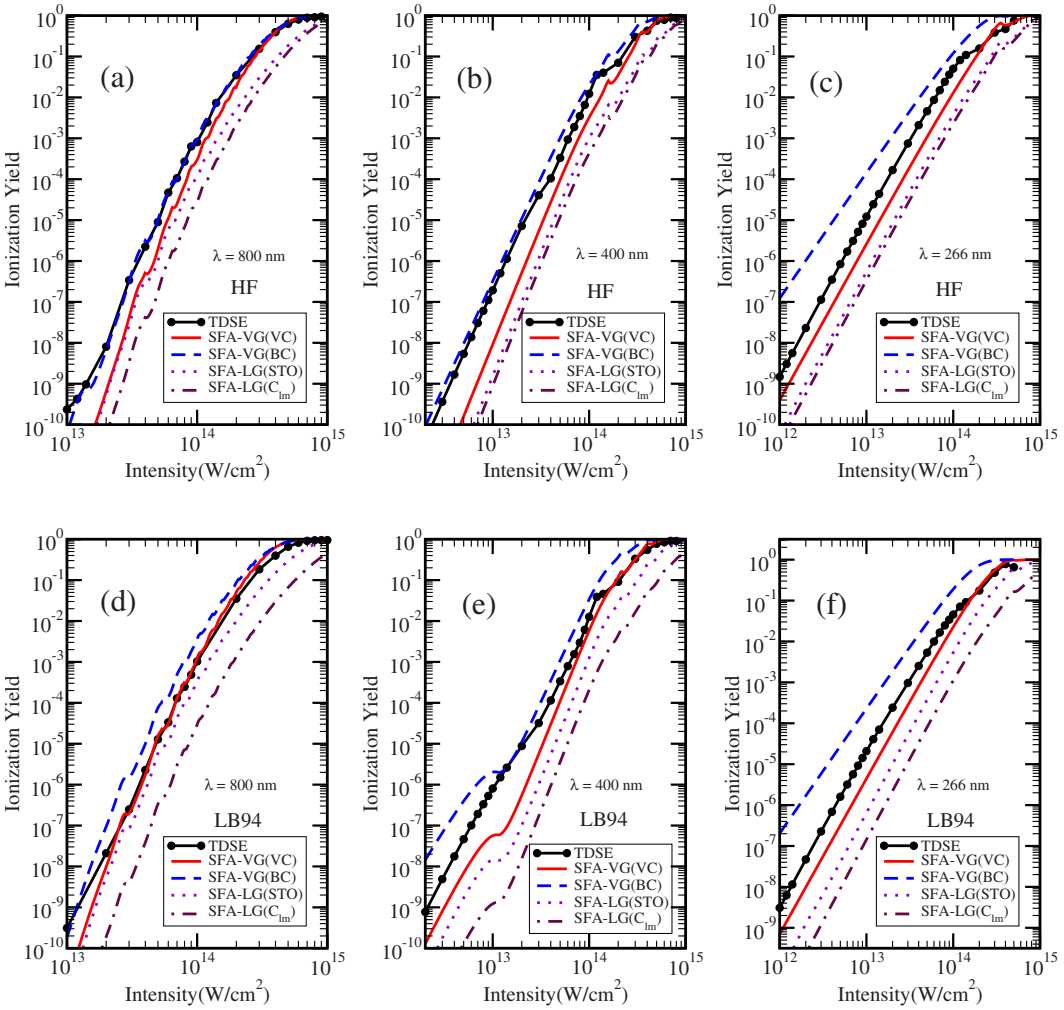

FIG. 10. (Color online) Ionization yield of H_2 for the same laser parameters as in Figs. 3 [800 nm, (a) and (d)], 5 [400 nm, (b) and (e)], and 7 [266 nm, (c) and (f)]. The SAE-TDSE results (black circles) are compared on one hand to the predictions of MO-SFA-VG using either the Coulomb-correction factor of Becker *et al.* [45] (BC, blue dashes) or the one of Vanne and Saenz [44] (VC, red solid) and on the other hand to the MO-SFA-LG results (without Coulomb-correction factor) that were obtained using either the complete HOMO expressed in an STO basis (STO, purple dots) or an approximate formula based on the C_{lm} coefficients (C_{lm}, maroon chain).

worse than MO-SFA-VG(BC). The simplified MO-SFA-LG (C_l) leads again to a pronounced underestimation of the yield, but agrees in shape relatively well with the full MO-SFA-LG(STO) curve.

It should be reminded that in view of the difference in molecular parameters (ionization potential and C_l coefficients, see Table I) the good agreement of the SAE-TDSE results for the HF and LB94 functionals was not expected. At first glance it appears as if the differences in the initial state are to a large extent compensated by corresponding differences in excitation energies and dipole transition moments. Since SFA depends only on the initial state and ignores all possible intermediate states, its larger sensitivity to differences in the initial state compared to SAE-TDSE could be explained this way. However, also MO-ADK depends only on the initial state, but the results obtained with either the HF or LB94 functional agree much better than for MO-SFA (but less well than it is the case for SAE-TDSE). Within the MO-SFA models, the best agreement for HF and LB94 models is found for MO-SFA-LG (C_l). This seems to indicate that in the long-range asymptotic behavior of the initial state the quantities ionization potential and C_l coefficients may partly compensate each other. In view of the fact that in the fit procedure that yields the C_l coefficients I_p is explicitly used, such a compensation may be understandable. This compensation can explain the better agreement of the yields for the HF and LB94 functionals when adopting a strong-field model that depends practically only on the asymptotic behavior of the initial-state wave function, as is the case for MO-ADK and MO-SFA-LG (C_l).

At 400 nm [Fig. 10(e)] the analysis is more complicated due to the occurrence of a pronounced channel closing in all MO-SFA yields at about 10^{13} W cm^{-2} that occurs only for the LB94 model, since the higher I_p obtained in the HF model would require correspondingly higher intensities for the channel closing to occur. Remind, however, that in the SAE-TDSE calculation an almost identical channel-closing intensity of 10^{14} W cm^{-2} is found for the HF and LB94 functionals, as was discussed earlier. A further interesting issue is that close to saturation the structure of the SAE-

TDSE yield appears to be reproduced by MO-SFA-VG using the HF functional, but it is completely absent when using the LB94 functional. In the case of MO-SFA-LG this structure is absent independent of the underlying electronic-structure model (HF or LB94), but also at this wavelength one notices that the LB94 model leads to a smaller slope compared to the HF model close to saturation.

This effect is even more evident for the results obtained for 266 nm [Fig. 10(f)]. At this wavelength the MO-SFA-VG results obtained with the HF or LB94 functional agree on the other hand quite well. This is in agreement with a multiphoton picture in which the transition probabilities depend less on the ionization potential and the asymptotic long-range behavior of the initial state than for tunneling and thus for longer wavelengths. Furthermore one notices that the simplified MO-SFA-LG approximation based on the C_l coefficients fails more clearly for the LB94 functional than for the HF functional. In both cases it is, however, dominantly a failure in absolute value while the shape of all MO-SFA-LG curves is very similar. In fact, the shape of MO-SFA-LG is in most cases in very good agreement to the one of MO-SFA-VG(VC). This agreement is, however, better for 400 and 266 nm than for 800 nm. In the latter case the slope of MO-SFA-LG is less steep. As a consequence one may conclude that a possible Coulomb-correction factor for MO-SFA-LG should be rather independent on the laser intensity, in contrast to the ones used in MO-SFA-VG(BC) or MO-SFA-VG(VC). There may, on the other hand, be the need for some wavelength dependence of such a factor, since for 800 nm the slope of the intensity curve obtained with MO-SFA-LG without Coulomb correction appears to be to small.

A criterion for the validity of the SFA depends (for a given system and thus a fixed ionization potential) on intensity and wavelength, as is also reflected, e.g., by the Keldysh parameter. In fact, one proposed validity criterion for SFA is $z_1 \gg 1$ with $z_1 = \gamma^{-2} = 2U_p/I_p$ [52,53]. Although it appears that at least for the total ion yields obtained with Coulomb-corrected MO-SFA-VG this validity criterion is too strict, the increasing failure of SFA with decreasing wavelength is correctly predicted by this parameter. Nevertheless, it is quite surprising how well the slope of the curves is predicted even for 266 nm and low intensities by MO-SFA [except MO-SFA-VG(BC)].

In conclusion, it is found that MO-SFA is in the nonresonant case more sensitive to the adopted electronic-structure model than SAE-TDSE, especially for longer wavelengths. In the considered examples, the SAE-TDSE results are essentially bracketed by MO-SFA-VG(BC) and MO-SFA-VG(VC). The latter gives the overall best agreement to SAE-TDSE with respect to both qualitative and quantitative agreement, but MO-SFA-VG(BC) is clearly superior for 800 and 400 nm, if the HF model is used. At 266 nm the Coulomb correction by Becker *et al.* leads to an evident failure of MO-SFA-VG(BC). MO-SFA-LG (without Coulomb correction) leads to a systematic underestimation of the ionization yield that appears to increase with descreasing wavelength. On the other hand, MO-SFA-LG yields a very good qualitative agreement with SAE-TDSE, especially for shorter wavelengths, where it also agrees rather well in shape with MO-SFA-VG(VC). The simplified MO-SFA-LG (C_l) model should be used with care, since its validity (in reproducing MO-SFA-LG) depends on the laser parameters wavelength and intensity as well as on the adopted electronic structure model. In all considered cases it underestimates the MO-SFA-LG yields that are themselves already too low compared to SAE-TDSE.

V. CONCLUSION AND OUTLOOK

A theoretical description of the response of molecular systems to intense short laser pulses has been developed and implemented in this work. It is based on the SAE approximation and describes all but one electron within DFT. The resulting time-dependent one-electron Schrödinger equation describing the selected electron in the combined field of the frozen core and the laser pulse is solved numerically using an expansion in field-free eigenstates. It is important to note that the present approach is not time-dependent density-functional theory (TD-DFT). The latter model describes the motion of all electrons in the laser field and is thus an alternative to more expensive many-electron treatments like time-dependent variants of Hartree-Fock, multiconfiguration Hartree- or Hartree-Fock, CI, etc. TD-DFT has, however, its own problems, especially related to the read-out of observables such as the ionization yields (see, e.g., part V in [54]).

The developed approach was applied to molecular hydrogen and the calculated total ion and excitation yields were compared to a full two-electron (CI) calculation. For high photon frequencies and relatively low intensities it was demonstrated that the SAE model predicts reasonable results for the dependence of ionization and excitation on the photon frequency. However, due to the pronounced structure of the spectrum and the sensitivity of it on the ionization and excitation energies, the SAE results at a given photon energy may deviate drastically from the correct yields. In the weakly perturbative regime this failure can be compensated to a large extent by rescaling the photon frequency.

For the popular Ti:sapphire laser wavelength of about 800 nm the intensity dependence of the ion yield obtained with different DFT functionals was investigated. From the tested ones, only the LB94 and HF functionals gave satisfactory results. In fact, the results obtained in these two cases agreed very well with each other and with the CI results. The agreement to CI is improved if a factor of 2 is adopted for laser intensities for which the ion yields are smaller than about 10%. This factor should reflect the two equivalent electrons. The predicted excitation yield is also in reasonable agreement with the CI result, but here the agreement becomes even less good for high peak intensities for which the SAE models strongly overestimate excitation. Clearly, by construction SAE models do not account for double excitation or even double ionization.

At smaller wavelengths the spectra are more sensitive to structural details. At the considered photon energies that correspond to the second and third harmonics of the 800 nm radiation the erroneously predicted ionization energy of H_2 using especially the LB94 model leads to channel-closing effects in the ion yield that are shifted in intensity compared to the CI result. The structural effects are much more pro-

nounced in the excitation spectra and lead to differences between SAE and CI that can easily exceed some orders of magnitude.

In those cases where the HF and LB94 results differed, the HF results are usually in better overall agreement with CI. This should be a consequence of the well-known problem of DFT to describe systems with a very small number of electrons like atomic or molecular hydrogen. The failure of the LB94 model to describe H_2 is already apparent from the poor ionization potential obtained with this approach. In fact, the very good overall agreement between the HF and LB94 models is somewhat surprising in view of these differences. With increasing size of the molecular system one should, however, expect that the present DFT-based approach should be superior to the HF model, since DFT is known to provide a very efficient way for a reliable description for a large number of many-electron molecules. An advantage of DFT in comparison to the HF model is the possibility to include to some extent correlation into the calculation. In the context of molecules in intense laser fields a prominent example for this advantage is given by molecular nitrogen. While the HF model predicts a wrong ordering of the orbitals and thus of the highest-occupied one, DFT predicts the correct ordering, as was also verified with the present code. More sophisticated functionals (such as LDA with self-interaction correction or exact-exchange within the optimized effective potential method) could be implemented in the future. The use of more sophisticated potentials does not increase the computational load of the time-propagation part of the calculation that is computationally most demanding, and is therefore merely a coding task.

The intensity-dependence of the ionization yield of H_2 predicted by MO-ADK is found to be in very poor agreement with SAE-TDSE, even at the longest wavelength (800 nm) considered in this work. There are not only quantitative deviations, but also the slope of the curves differ considerably. Since it has been shown earlier that for field strengths lower than the classical threshold for over-the-barrier ionization, ADK predicts absolute *dc-field* ionization rates of H_2 in very good agreement with a full complex-scaling based *ab initio* CI calculation [55,56], the observed failure of MO-ADK is due to a breakdown of the quasistatic approximation. This failure may not appear surprising in view of the fact that based on the analysis of the Keldysh parameter and classical over-the-barrier ionization threshold limit the applicability of a tunneling model like ADK should be limited to a very small range of intensities. However, the present work provides a quantitative description of the failure of MO-ADK to approximate the SAE-TDSE result. This is very important, since MO-ADK was frequently used outside its parameter range of validity, for example, in the context of suppressed ionization. The present work shows that such an analysis is very problematic.

The MO-SFA-VG approach gives (on a double-logarithmic scale) reasonable agreement with SAE-TDSE results if a Coulomb-correction factor is employed. It should be reminded that this factor is not at all small, but typically of the size of one to three orders of magnitude. The ion yields obtained with MO-SFA-VG using the two proposed factors by Becker *et al.* (BC) and Vanne and Saenz (VC) lead to a bracketing of the SAE-TDSE results, since MO-SFA-VG(BC) tends to overestimate the yield while MO-SFA-VG(VC) tends to underestimate it. Furthermore, MO-SFA-VG turns out to be much more sensitive to the employed electronic-structure model (Hartree-Fock vs density-functional theory with LB94 functional) than SAE-TDSE. This leads to the surprising (and probably accidental) result that especially at 800 nm MO-SFA-VG(BC) leads to an almost perfect agreement with SAE-TDSE in the case of HF, while MO-SFA-VG(VC) provides an almost perfect agreement in the case of DFT (LB94). At 266 nm MO-SFA-VG(VC) gives good qualitative agreement with SAE-TDSE for lower intensities and even almost quantitative agreement for very high ones. On the other hand, the Coulomb correction of Becker *et al.* fails rather badly at this wavelength. Since it was empirically found from data that dominantly come from longer wavelengths, this result is not completely unexpected. It indicates, however, a principal shortcoming of this Coulomb-correction factor, since it is not universal. Also the Coulomb-correction factor of Vanne and Saenz is not derived for arbitrary wavelengths, but stems from the requirement that the SFA results should converge for $\omega \rightarrow 0$ to the tunneling result. Although the correction factor is proportional to ω (while the BC factor is ω independent), there is clearly no reason to believe that this factor works for arbitrary wavelengths. In view of the results obtained in this work for 800, 400, and 266 nm this factor leads, however, finally to the best overall agreement. Surprisingly, it works well for low intensities and wavelengths, and thus in a limit that is absolutely contrary to the tunnel limit in which it was derived.

The shape of the yield curves obtained with MO-SFA-LG without Coulomb correction is typically very similar to the one obtained with MO-SFA-VG(VC). Thus it shows similar relative deviations to SAE-TDSE, but is quantitatively too low. In comparison to SAE-TDSE one may conclude that a possible Coulomb-correction factor for MO-SFA-LG should be rather independent of the intensity (except possibly for longer wavelengths), since otherwise the good agreement in shape would be lost. The simplified version of MO-SFA-LG based on the asymptotic C_l coefficients was found to yield ionization yields that agree in shape rather well with the full MO-SFA-LG results, but leads to a further underestimation. It should also be reminded that in contrast to SAE-TDSE none of the simplified SAE models MO-ADK or MO-SFA can predict excitation to electronic bound states. Especially for smaller wavelengths excitation is found to be very important.

Future work will investigate the orientational dependence of the ionization yield of H_2 as well as differential quantities like photoelectron spectra. Also high-harmonic spectra of H_2 calculated with either CI-TDSE, SAE-TDSE, or MO-SFA will be investigated. The main future work will, however, be devoted to larger molecular systems. First results for systems as large as acetylene have already been obtained and will be discussed elsewhere. While the validity of the SAE itself for such systems can, of course, in principle only be determined from corresponding full-electron calculations that appear presently out of reach, the present approach should allow one to not only investigate the validity of MO-ADK and

MO-SFA for such systems, but to provide an alternative treatment with only a single unknown, the validity of the SAE itself. This is of great interest, since the exact range of validity of MO-ADK and MO-SFA is so far unknown. A great advantage compared to SFA is also the gauge independence of the results obtained with SAE-TDSE. Furthermore, as the present work has confirmed, for quantitative predictions the MO-SFA models require the knowledge of a Coulomb correction. Whether a simple correction factor valid for all laser-parameter regimes and molecules exists is completely unclear. None of the tested factors leads to fully convincing results. It should also be emphasized that H_2 may be not the most representative case, since it possesses for a molecule a rather isotropic electron density that is furthermore nodeless. Therefore simplified models may work better in this case than for molecules with more complicated structure. The reasonable success of the two Coulomb-correction factors discussed for MO-SFA-VG may be partly due to the similarity to atomic hydrogen.

ACKNOWLEDGMENTS

A.S. acknowledges financial support by Stifterverband für die Deutsche Wissenschaft and the Fonds der Chemischen Industrie. Support provided by the Deutsche Forschungsgemeinschaft within Projects No. DFG-Sa 936/2 (M.A. and A.S.) and No. SFB 658 (A.C.) is also acknowledged. A.S. and P.D. acknowledge support by the European COST Programme D26/0002/02 and A.C. by the 6th EU Framework Programme through NANOQUANTA NoE.

[1] J. H. Posthumus, Rep. Prog. Phys. **67**, 623 (2004).
[2] J. Muth-Böhm, A. Becker, and F. H. M. Faisal, Phys. Rev. Lett. **85**, 2280 (2000).
[3] F. Grasbon, G. G. Paulus, S. L. Chin, H. Walther, J. Muth-Böhm, A. Becker, and F. H. M. Faisal, Phys. Rev. A **63**, 041402(R) (2001).
[4] I. V. Litvinyuk, K. F. Lee, P. W. Dooley, D. M. Rayner, D. M. Villeneuve, and P. B. Corkum, Phys. Rev. Lett. **90**, 233003 (2003).
[5] G. Lagmago Kamta and A. D. Bandrauk, Phys. Rev. A **70**, 011404(R) (2004).
[6] T. K. Kjeldsen, C. Z. Bisgaard, L. B. Madsen, and H. Stapelfeldt, Phys. Rev. A **71**, 013418 (2005).
[7] A. Saenz, J. Phys. B **33**, 4365 (2000).
[8] A. Saenz, Phys. Rev. A **66**, 063407 (2002).
[9] X. Urbain, B. Fabre, V. M. Andrianarijaona, J. Jureta, J. H. Posthumus, A. Saenz, E. Baldit, and C. Cornaggia, Phys. Rev. Lett. **92**, 163004 (2004).
[10] T. K. Kjeldsen and L. B. Madsen, Phys. Rev. Lett. **95**, 073004 (2005).
[11] A. Requate, A. Becker, and F. H. M. Faisal, Phys. Rev. A **73**, 033406 (2006).
[12] M. V. Ammosov, N. B. Delone, and V. P. Krainov, Sov. Phys. JETP **64**, 1191 (1986).
[13] A. Talebpour, C.-Y. Chien, and S. L. Chin, J. Phys. B **29**, L677 (1996).
[14] C. Guo, M. Li, J. P. Nibarger, and G. N. Gibson, Phys. Rev. A **58**, R4271 (1998).
[15] S. M. Hankin, D. M. Villeneuve, P. B. Corkum, and D. M. Rayner, Phys. Rev. Lett. **84**, 5082 (2000).
[16] J. Wu, H. Zeng, and C. Guo, Phys. Rev. Lett. **96**, 243002 (2006).
[17] X. M. Tong, Z. X. Zhao, and C. D. Lin, Phys. Rev. A **66**, 033402 (2002).
[18] T. K. Kjeldsen and L. B. Madsen, Phys. Rev. A **71**, 023411 (2005).
[19] T. K. Kjeldsen and L. B. Madsen, J. Phys. B **37**, 2033 (2004).
[20] T. K. Kjeldsen and L. B. Madsen, Phys. Rev. A **73**, 047401 (2006).
[21] A. Jaroń-Becker, A. Becker, and F. H. M. Faisal, Phys. Rev. A **69**, 023410 (2004).
[22] V. I. Usachenko, Phys. Rev. A **73**, 047402 (2006).
[23] D. B. Milošević, Phys. Rev. A **74**, 063404 (2006).
[24] N. Rohringer, A. Gordon, and R. Santra, Phys. Rev. A **74**, 043420 (2006).
[25] K. C. Kulander, Phys. Rev. A **35**, 445 (1987).
[26] X. Tang, H. Rudolph, and P. Lambropoulos, Phys. Rev. A **44**, R6994 (1991).
[27] M. J. Nandor, M. A. Walker, L. D. Van Woerkom, and H. G. Muller, Phys. Rev. A **60**, R1771 (1999).
[28] R. Wiehle, B. Witzel, H. Helm, and E. Cormier, Phys. Rev. A **67**, 063405 (2003).
[29] A. Becker and F. H. M. Faisal, J. Phys. B **38**, R1 (2005).
[30] M. Lezius, V. Blanchet, D. M. Rayner, D. M. Villeneuve, A. Stolow, and M. Y. Ivanov, Phys. Rev. Lett. **86**, 51 (2001).
[31] T. Brabec, M. Côté, P. Boulanger, and L. Ramunno, Phys. Rev. Lett. **95**, 073001 (2005).
[32] V. R. Bhardwaj, P. B. Corkum, and D. M. Rayner, Phys. Rev. Lett. **91**, 203004 (2003).
[33] A. Jaroń-Becker, A. Becker, and F. H. M. Faisal, Phys. Rev. Lett. **96**, 143006 (2006).
[34] H. Kono, Y. Sato, N. Tanaka, T. Kato, K. Nakai, S. Koseki, and Y. Fujimura, Chem. Phys. **304**, 203 (2004).
[35] M. Awasthi, Y. V. Vanne, and A. Saenz, J. Phys. B **38**, 3973 (2005).
[36] M. Awasthi and A. Saenz, J. Phys. B **39**, S389 (2006).
[37] P. Lambropoulos, P. Maragakis, and J. Zhang, Phys. Rep. **305**, 203 (1998).
[38] D. Toffoli, M. Stener, G. Fronzoni, and P. Decleva, Chem. Phys. **276**, 25 (2002).
[39] E. J. Baerends, D. E. Ellis, and P. Ros, Chem. Phys. **2**, 41 (1973).
[40] G. Fonseca-Guerra, J. G. Snijders, G. te Velde, and E. J. Baerends, Theor. Chem. Acc. **99**, 391 (1998).
[41] M. Brosolo and P. Decleva, Chem. Phys. **159**, 185 (1992).
[42] G. F. Gribakin and M. Y. Kuchiev, Phys. Rev. A **55**, 3760 (1997).
[43] Y. V. Vanne and A. Saenz, Phys. Rev. A **75**, 033403 (2007).
[44] Y. V. Vanne and A. Saenz, Phys. Rev. A **75**, 063403 (2007).
[45] A. Becker, L. Plaja, P. Moreno, M. Nurhuda, and F. H. M.

Faisal, Phys. Rev. A **64**, 023408 (2001).
[46] P. Hohenberg and W. Kohn, Phys. Rev. **136**, B864 (1964).
[47] L. W. S. H. Vosko and M. Nusair, Can. J. Phys. **58**, 1200 (1980).
[48] R. van Leeuwen and E. J. Baerends, Phys. Rev. A **49**, 2421 (1994).
[49] M. E. McHenry, R. C. O'Handley, and K. H. Johnson, Phys. Rev. B **35**, 3555 (1987).
[50] M. Stener, S. Furlan, and P. Decleva, J. Phys. B **33**, 1081 (2000).
[51] Y. V. Vanne and A. Saenz, J. Phys. B **37**, 4101 (2004).
[52] H. R. Reiss, Phys. Rev. A **22**, 1786 (1980).
[53] H. R. Reiss, Phys. Rev. A **75**, 031404(R) (2007).
[54] *Time-Dependent Density Functional Theory*, edited by M. A. L. Marques, C. A. Ullrich, F. Nogueira, A. Rubio, K. Burke, and E. K. U. Gross (Springer, Berlin, 2006).
[55] A. Saenz, Phys. Rev. A **61**, 051402(R) (2000).
[56] A. Saenz, Phys. Rev. A **66**, 063408 (2002).